

## Bulk photonic metamaterial with hyperbolic dispersion

M. A. Noginov,<sup>1,a)</sup> Yu. A. Barnakov,<sup>1</sup> G. Zhu,<sup>1</sup> T. Tumkur,<sup>2,3</sup> H. Li,<sup>1</sup> and E. E. Narimanov<sup>4</sup>

<sup>1</sup>Center for Materials Research, Norfolk State University, Norfolk, Virginia 23504, USA

<sup>2</sup>Summer Research Program, Center for Materials Research, Norfolk State University, Norfolk, Virginia 23504, USA

<sup>3</sup>School of Materials Engineering, Purdue University, West Lafayette, Indiana 47907, USA

<sup>4</sup>School of Electrical Engineering, Purdue University, West Lafayette, Indiana 47907, USA

(Received 10 December 2008; accepted 15 March 2009; published online 14 April 2009)

We have demonstrated the thickest bulk photonic metamaterial reported in the literature based on an Ag-filled alumina membrane. The material is highly anisotropic with hyperbolic dispersion at  $\lambda > 0.84 \mu\text{m}$ . The refraction of light in the direction expected of isotropic media with  $n < 1$  has been experimentally demonstrated at  $\lambda = 632.8 \text{ nm}$ . This makes the material potentially suitable for a variety of applications ranging from subdiffraction imaging to optical cloaking. © 2009 American Institute of Physics. [DOI: 10.1063/1.3115145]

Photonic metamaterials are engineered nanocomposite structures with optimized responses to electromagnetic fields at optical frequencies that lead to superlens<sup>1</sup> and hyperlens<sup>2–5</sup> and invisibility cloaks,<sup>6–12</sup> bringing closer a variety of exciting applications and calling for inexpensive three-dimensional media. Most metamaterials are fabricated using prohibitively expensive nanolithography techniques and are available in a form of subwavelength thin films. Recent advances in nonlithographic fabrication include direct laser writing,<sup>13</sup> epitaxy,<sup>14</sup> self-organized<sup>15</sup> growth, and electroplating.<sup>16–18</sup> Here we demonstrate a self-standing 51- $\mu\text{m}$ -thick three-dimensional metamaterial based on a network of silver nanowires in an alumina membrane. This constitutes the anisotropic effective medium with hyperbolic dispersion,<sup>19</sup> which can be used in subdiffraction imaging<sup>20</sup> or optical cloaks.<sup>7</sup> Highly anisotropic dielectric constants of the material range from positive to negative, and the transmitted laser beam shifts both *toward* the normal to the surface, as in regular dielectrics, and *off* the normal, as in dielectrics with the refraction index smaller than one.

Anodic alumina membranes (AAMs) with dimensions  $1 \text{ cm} \times 1 \text{ cm} \times 51 \mu\text{m}$ , hole diameter equal to 35 nm and porosity equal to 15% have been acquired from Synkera Technologies, Inc. [Fig. 1(a)]. Silver nanowires were synthe-

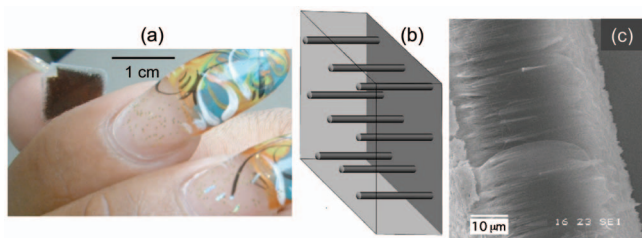


FIG. 1. (Color) (a) Photograph of the silver-filled membrane. (b) Schematic of silver nanowires in an alumina membrane. (Modified from Ref. 19.) (c) Scanning electron microscope picture of the etched side wall of the membrane showing loose silver nanowires.

sized in AAMs via electrochemical plating. A thin gold film ( $\sim 50 \text{ nm}$ ) deposited on the membrane's surface via thermal vapor deposition technique served as the working electrode and a graphite rod played a role of the counter electrode. A mixture of aqueous solutions of silver nitrate (1.76M) and boric acid (0.7M) buffered with nitric acid to pH 2–3 were used as an electrolyte. A dc voltage of 1 V was applied during  $\sim 300 \text{ min}$  deposition. The gold electrode was removed before the optical studies. The nanowires synthesized inside the membranes in this study were two orders of magnitude longer than the subwavelength nanorods reported in Refs. 16–18.

The membranes were almost completely filled with silver at the electrode side and the concentration of silver somewhat reduced toward the opposite side [Fig. 1(b)]. In the best samples, the dielectric constants  $\epsilon$  measured on both sides (determined from the reflectance studies described below) were close to each other, suggesting high uniformity of filling.

In the reflectance studies, the samples were mounted at the axis of rotation of a goniometer, where they were intercepted by a  $\sim 0.5 \text{ mm}$  laser beam. The sample's reflectance in *s* and *p* polarizations was measured as a function of the incidence angle at ten different wavelengths ranging from 458 to 950 nm [Fig. 2(a)]. The spectrum of the experimentally measured Brewster angles (angles of minimal reflectance)

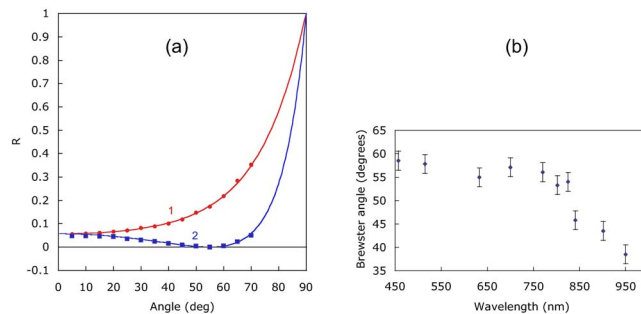


FIG. 2. (Color online) (a) The dependence of the reflectance on the incidence angle in *s* polarization (trace 1, circles) and *p* polarization (trace 2, squares) at  $\lambda = 632.8 \text{ nm}$ . Solid lines—calculation according to Eq. (1). The scattering factor is taken into account. (b) The summary of the experimentally measured Brewster angles.

<sup>a)</sup>Author to whom correspondence should be addressed. Electronic mail: mnoginov@nsu.edu. Tel.: (757) 823 2204.

tance in *p* polarization) [Fig. 2(b)], shows a discontinuity at the wavelength ( $\lambda=0.84 \mu\text{m}$ ) at which the dielectric constant in the direction perpendicular to the membrane's surface changes its sign from positive to negative, as shown in Fig. 3 and explained below. This pattern is qualitatively similar to that predicted theoretically and observed

$$R = |r|^2 = \begin{cases} \left| \frac{\sin(\theta - \theta_t)}{\sin(\theta + \theta_t)} \right|^2, & \theta_t = \arcsin\left(\frac{\sin \theta}{\sqrt{\epsilon_{\parallel}}}\right), & s \text{ polarization,} \\ \left| \frac{\epsilon_{\parallel} \tan \theta_t - \tan \theta}{\epsilon_{\parallel} \tan \theta_t + \tan \theta} \right|^2, & \theta_t = \arctan \sqrt{\frac{\epsilon_{\perp} \sin^2 \theta}{\epsilon_{\parallel} \epsilon_{\perp} - \epsilon_{\parallel} \sin^2 \theta}}, & p \text{ polarization.} \end{cases} \quad (1)$$

We first determined the values  $\epsilon_{\parallel}$  by fitting the reflectance in *s* polarization. A relatively small but noticeable amount of light was scattered diffusely. Consequently, the agreement between the fitting and the experiment strongly improved if the experimental data (in both polarizations) were scaled by a constant on the order of unity. Keeping  $\epsilon_{\parallel}$  and the scattering factor unchanged, we then used  $\epsilon_{\perp}$  as a variable parameter to fit the reflectance in *p* polarization. In the fitting procedure, we were mainly concerned with the position of the Brewster angle, since this parameter was experimentally known with the highest accuracy. In the two-step fitting procedure, the accuracy of  $\epsilon_{\parallel}$  was higher than the accuracy of  $\epsilon_{\perp}$ . The reflectance curves were much more sensitive to real than to imaginary parts of  $\epsilon$ . That is why only real parts of the dielectric constants, shown in Fig. 3, have been determined. According to transmission measurements carried out in an integrating sphere setup at normal angle of incidence, the figure of merit (the ratio of real to imaginary parts of the index of refraction) for the direction parallel to the membrane surface exceeds 530 over the whole spectral range studied. This is consistent with the small effect of the imaginary part of  $\epsilon$  on the shape of the reflectance curves.

As expected, the synthesized metamaterial is highly anisotropic, with  $\epsilon_{\perp}$  changing sign from positive to negative at the wavelength of the discontinuity of the Brewster angle [Fig. 2(b)]. According to Ref. 19, in a silver-filled alumina membrane  $\epsilon_{\parallel}$  is predicted to be positive and changes slowly in the wavelength range studied, while  $\epsilon_{\perp}$  is expected to change sign at  $\sim 0.84 \mu\text{m}$  at the value of the filling factor

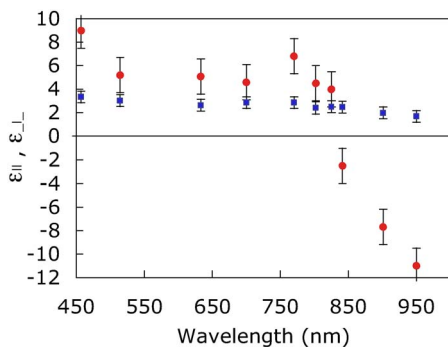


FIG. 3. (Color online) Real parts of  $\epsilon_{\parallel}$  (squares) and  $\epsilon_{\perp}$  (circles) determined from the reflectance measurements.

experimentally<sup>14</sup> in the multilayered sandwich structure of doped  $\text{In}_{0.53}\text{Ga}_{0.47}\text{As}$  and undoped  $\text{Al}_{0.48}\text{In}_{0.52}\text{As}$  semiconductor layers, which obeyed a hyperbolic dispersion law and demonstrated negative refraction of *p*-polarized light.

The experimental curves were fitted with the known theoretical expressions for reflection from a uniaxial material<sup>14</sup>

equal to  $\sim 8\%$ . The discrepancy of the filling factors, 15% versus 8%, can be explained by imperfect electroplating or the difference in properties of bulk silver<sup>21</sup> and the silver deposited into the membrane.

Angles of refraction for both *p*- and *s*-polarized light were directly studied in silver-filled membranes at  $\lambda = 632.8 \text{ nm}$  in the modified knife edge setup of Ref. 14 [Fig. 4(a)]. First, the sample was positioned normally to the laser beam ( $d \approx 0.15 \text{ mm}$ ) and the dependence of the transmitted intensity on the knife edge position was measured [Fig. 4(b)]. Then, the knife edge was moved to the position where it blocked  $\sim 50\%$  of the transmitted light. After that, the sample was rotated and depending on the angle of refraction and the direction of rotation, the amount of light measured after the knife edge increased or decreased by a certain value [Figs. 4(a) and 4(b)].

The silver-filled membranes were scattering. This contributed to the relatively large scatter of transmitted intensities [Fig. 4(b)], which was stronger in filled membranes than in pure membranes or in the thin glass slide. To reduce the scatter of the data, the transmitted intensities in Fig. 4(b),

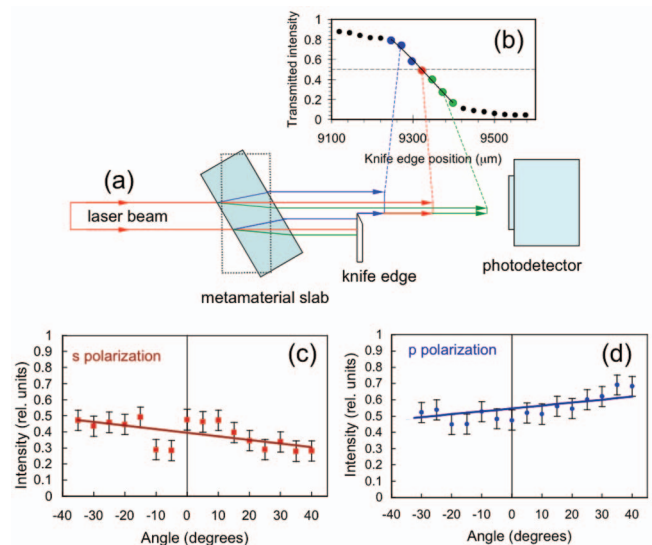


FIG. 4. (Color) (a) Experimental setup used at the beam shift measurements. (b) Beam profile measured with the knife edge technique; [(c) and (d)] shifts in opposite directions for *s* and *p* polarizations.

measured after the knife edge, were normalized to those measured at the same angles without the knife edge.

We have shown that in *s* polarization, the directions of the beam shifts, as indicated by changes in the measured light intensity, were the same as in thin glass slide with the index of refraction *n* greater than one [Fig. 4(c)]. At the same time, at *p* polarization, the beam shifted in the opposite direction [Fig. 4(d)]. In isotropic media, such a situation would correspond to  $n < 1$ . This is another demonstration of the strong anisotropy of the synthesized metamaterial.

Dielectric constants greater than zero and smaller than one are needed in optical cloaks. This makes the developed silver-filled membranes promising for cloaking applications, in particular if the cylindrical geometry (“hair brush” structures<sup>7</sup>) can be achieved. The same geometry with the hyperbolic law of dispersion would be ideal for the realization of a hyperlens.<sup>20</sup>

To summarize, we have demonstrated bulk photonic metamaterial based on anodized alumina membranes filled with silver. The material is highly anisotropic and follows the hyperbolic dispersion law at  $\lambda > 0.84 \mu\text{m}$ . The refraction of light in the direction expected of isotropic media with  $n < 1$  has been experimentally demonstrated at  $\lambda = 632.8 \text{ nm}$ . The designed photonic metamaterial is the thickest reported in the literature, both in terms of its physical size  $d = 51 \mu\text{m}$  and the number of vacuum wavelengths  $N = 61$  at  $\lambda = 0.84 \mu\text{m}$  and  $n = 81$  at  $\lambda = 0.63 \mu\text{m}$ . This combination of unique properties makes the material suitable for a variety of applications ranging from subdiffraction imaging to optical cloaking. When the experimental work was completed,<sup>22</sup> a paper was published<sup>23</sup> reporting negative refraction in thinner membranes  $d \leq 11 \mu\text{m}$ .

The work was supported by the NSF PREM Grant No. DMR 0611430, NSF CREST Grant No. HRD 0317722, NSF NCN Grant No. EEC-0228390, NASA URC Grant No. NCC3-1035, and ARO-MURI Award No. 50342-PH-MUR. The authors thank Viktor A. Podolskiy for useful discussions

and Natalia Noginova for the help with the data processing. Carla S. McKinney holds the sample in Fig. 1(a).

- <sup>1</sup>J. B. Pendry, *Phys. Rev. Lett.* **85**, 3966 (2000).
- <sup>2</sup>Z. Jacob, L. V. Alekseyev, and E. E. Narimanov, *Opt. Express* **14**, 8247 (2006).
- <sup>3</sup>A. Salandrino and N. Engheta, *Phys. Rev. B* **74**, 075103 (2006).
- <sup>4</sup>Z. Liu, H. Lee, Y. Xiong, C. Sun, and X. Zhang, *Science* **315**, 1686 (2007).
- <sup>5</sup>I. I. Smolyaninov, Y.-J. Hung, and C. C. Davis, *Science* **315**, 1699 (2007).
- <sup>6</sup>J. B. Pendry, D. Schurig, and D. R. Smith, *Science* **312**, 1780 (2006).
- <sup>7</sup>W. Cai, U. K. Chettiar, A. V. Kildishev, and V. M. Shalaev, *Nat. Photonics* **1**, 224 (2007).
- <sup>8</sup>G. W. Milton and N. A. P. Nicorovici, *Proc. R. Soc. London, Ser. A* **462**, 3027 (2006).
- <sup>9</sup>A. Alu and N. Engheta, *Phys. Rev. E* **72**, 016623 (2005).
- <sup>10</sup>F. J. Garcia de Abajo, G. Gómez-Santos, L. A. Blanco, A. G. Borisov, and S. V. Shabanov, *Phys. Rev. Lett.* **95**, 067403 (2005).
- <sup>11</sup>D. A. B. Miller, *Opt. Express* **14**, 12457 (2006).
- <sup>12</sup>U. Leonhardt, *Science* **312**, 1777 (2006).
- <sup>13</sup>M. S. Rill, C. Plet, M. Thiel, I. Staude, G. Von Freymann, S. Linden, and M. Wegener, *Nature Mater.* **7**, 543 (2008).
- <sup>14</sup>A. J. Hoffman, L. Alekseev, S. S. Howard, K. J. Franz, D. Wasserman, V. A. Podolskiy, E. E. Narimanov, D. L. Sivco, and C. Gmachl, *Nature Mater.* **6**, 946 (2007).
- <sup>15</sup>D. A. Pawlak, *Shaped Crystals*, Advances in Materials Research Vol. 8, (Springer, Berlin, Heidelberg, 2007), pp. 129–139.
- <sup>16</sup>P. R. Evans, G. A. Wurtz, R. Atkinson, W. Hendren, D. O’Connor, W. Dickson, R. J. Pollard, and A. V. Zayats, *J. Phys. Chem. C* **111**, 12522 (2007).
- <sup>17</sup>W. Dickson, G. A. Wurtz, P. Evans, D. O’Connor, R. Atkinson, R. Pollard, and A. V. Zayats, *Phys. Rev. B* **76**, 115411 (2007).
- <sup>18</sup>G. A. Wurtz, W. Dickson, D. O’Connor, R. Atkinson, W. Hendren, P. Evans, R. Pollard, and A. V. Zayats, *Opt. Express* **16**, 7460 (2008).
- <sup>19</sup>J. Elser, R. Wangberg, V. A. Podolskiy, and E. E. Narimanov, *Appl. Phys. Lett.* **89**, 261102 (2006).
- <sup>20</sup>Z. Jacob, L. V. Alekseev, and E. E. Narimanov, *Opt. Express* **14**, 8247 (2006).
- <sup>21</sup>D. W. Lynch and W. R. Hunter, in *Handbook of Optical Constants of Solids, Part II*, edited by E. D. Palik (Academic, New York, 1985).
- <sup>22</sup>M. A. Noginov, Yu. A. Barnakov, G. Zhu, T. Tumkur, H. Li, and E. E. Narimanov, e-print arXiv:0809.1028.
- <sup>23</sup>J. Yao, Z. Liu, Y. Liu, Y. Wang, C. Sun, G. Bartal, A. M. Stacy, and X. Zhang, *Science* **321**, 930 (2008).